

Supporting Information

Solvent Modulated Excited State Processes of Push-Pull Molecule with Hybridized Local Excitation and Intramolecular Charge Transfer Character

*Hongwei Song,^{ab} Kang Wang,^{ab} Zhuoran Kuang,^{ab} Yong Sheng Zhao^{ab}, Qianjin Guo,^{*a} Andong Xia,^{*ab}*

^aBeijing National Laboratory for Molecular Sciences (BNLMS), Key Laboratory of Photochemistry, Institute of Chemistry, Chinese Academy of Sciences, Beijing 100190, People's Republic of China

^bUniversity of Chinese Academy of Sciences, Beijing 100049, People's Republic of China

Main Contents

- S1. Details of the transient absorption spectra.
- S2. Lippert-Mataga analysis of CNDPASDB.
- S3. Solvation effects on fluorescence quantum yield and lifetime.
- S4. Electronic-State Transitions and Frontier Orbitals of CNDPASDB in Gas Phase and ACN.
- S5. Time-resolved TA spectra in cyclohexane of CNDPASDB following 400 nm photoexcitation.
- S6. Lifetime measurement at selected wavelength of CNDPASDB in THF.
- S7. The coupling deactivation pathways in medium-polarity solvent THF.

S1. Details of the transient absorption spectra.

Transient absorption measurements with a time resolution of ~90 fs were performed by using a homemade femtosecond broadband pump-probe setup. Briefly, a regeneratively amplified Ti:sapphire laser (Coherent Legend Elite) produced 40 fs, 500 Hz repetition rate, 1 mJ pulses at ~800 nm (FWHM: 30 nm). Doubling 90 percent of initial 800nm pulses through a 0.5 mm thick BBO (type I) crystal generated the 400 nm pump pulse. The rest of the 800 nm pulse was time-delayed by a computer-controlled optical delay line and then focused onto a 2 mm-thick water cell to produce a white light continuum (WLC), which provides a usable probe spectral range between 420 nm and 950 nm selected by a bandpass filter. The white light continuum was further split into two beams as the reference and signal beams by a broadband 50/50 beamsplitter. The pump and signal beams were overlapped in time and space on a sample cell with a 1 mm beam path length, and the reference beam passed through the unexcited part of the sample. The pump power is about 70 nJ/pulse (spot size of ~ 120 μm in each case) during transient absorption measurements. Signal and reference beams were detected on a fiber-coupled dual-channel spectrometer (Avantes AvaSpec-2048-2-USB2).

S2.Lippert-Mataga analysis of CNDPASDB.

The difference between the ground and excited state dipole moments can be calculated by the commonly used Lippert-Mataga equation:

$$\nu_a - \nu_f = \frac{1}{4\pi\epsilon_0} \frac{2}{hca^3} (\mu_e - \mu_g)^2 \Delta f + \text{const} \quad (\text{S1})$$

Where h is Planck's constant, ϵ_0 is the vacuum permittivity, Δf is the orientation polarizability of solvents, c is the speed of light in vacuum, ν_a and ν_f represent the maximum absorbance and fluorescence wavenumber, respectively, μ_e and μ_g are the dipole moments of the emitting excited state and ground state, respectively. a is the radius of corresponding spherical Onsager volume of the solute molecule (7.0 Å), and here estimated from the quantum-chemical calculations using the density functional theory method at the B3LYP/6-31G(d,p) level.

The orientation polarizability is defined as:

$$\Delta f = \frac{\varepsilon-1}{2\varepsilon+1} - \frac{n^2-1}{2n^2+1} \quad (\text{S2})$$

Where ε is the polarity and n is the optical refractive index of the solvents. Equation (S1) correspond to a linear expression $\Delta\nu=f(\Delta f)$ with a slope k from which $\Delta\mu^2$ can be calculated according to:

$$\Delta\mu^2 = 2\pi\varepsilon_0 h c a^3 \cdot k \quad (\text{S3})$$

From the figure 2 we obtain the slope in low-polarity solvents $k=0.32 \times 10^6 \text{ m}^{-1}$, and in high-polarity solvents $k=2.1 \times 10^6 \text{ m}^{-1}$. Using eq. S3 together with the standard constants given below one obtains a value of $\Delta\mu_{low}^2=1.20 \times 10^{-57} \text{ A}^2\text{s}^2\text{m}^2$ and $\Delta\mu_{high}^2=7.93 \times 10^{-57} \text{ A}^2\text{s}^2\text{m}^2$, $\Delta\mu_{low}=10.5\text{D}$, $\Delta\mu_{high}=26.9\text{D}$. $c = 2.9997 \times 10^8 \text{ ms}^{-1}$, $h = 6.6 \times 10^{-34} \text{ Js}$; $\varepsilon = 8.85 \times 10^{-12} \text{ CV}^{-1}\text{m}^{-1}$; 1 Debye = $3.3 \times 10^{-30} \text{ Cm}$.

S3. Solvation effects on fluorescence quantum yield and lifetime.

As shown in Table 2, the fluorescence properties are sensitive to the polarity of solvents. Fig. S1 shows the fluorescence lifetimes of **CNDPASDB** in different solvents by time-correlated single photon counting (TCSPC) measurements.

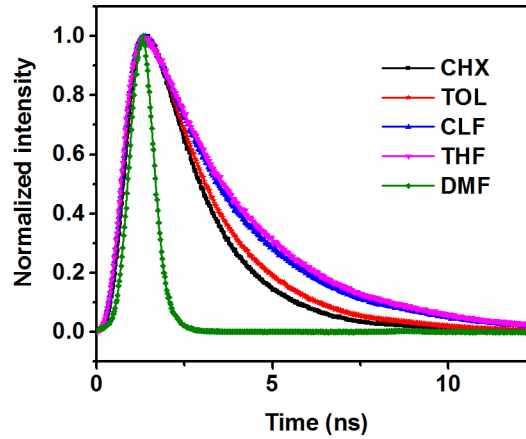


Figure S1. Fluorescence lifetimes of **CNDPASDB**. Fitting results are listed in Table 2.

The radiative and nonradiative rate constants k_r and k_{nr} are calculated from the measured quantum yield (Φ_f) and lifetime (τ_f) as based on equation S4 and S5:

$$k_r = \Phi_f / \tau_f \quad (\text{S4})$$

$$k_{nr} = 1/\tau_f - k_r \quad (\text{S5})$$

S4. Electronic-State Transitions and Frontier Orbitals of CNDPASDB in Gas Phase and ACN.

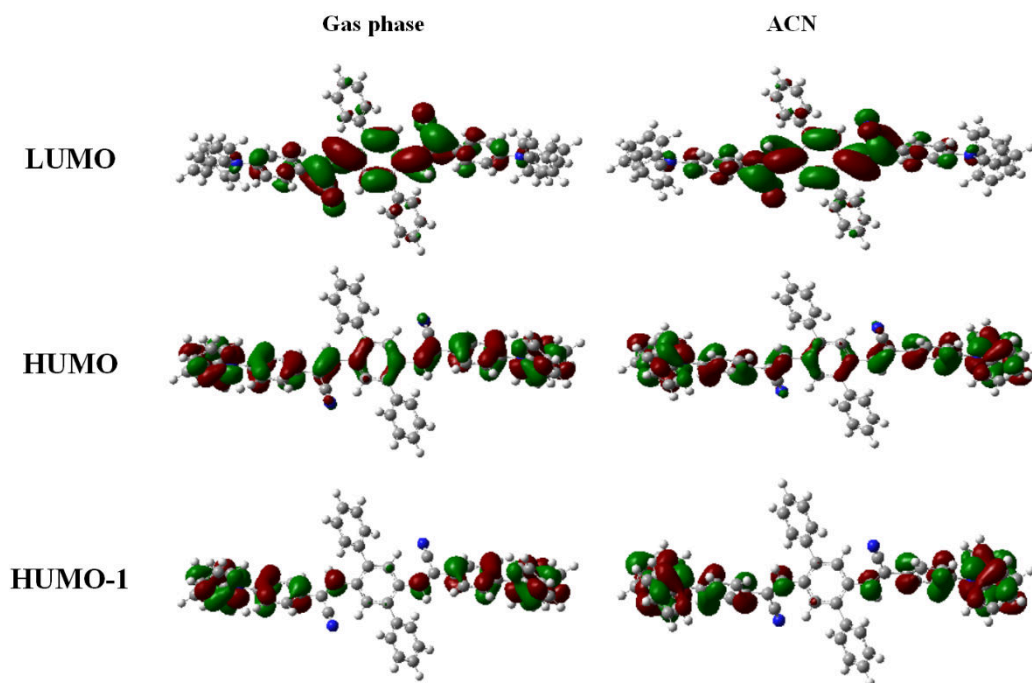


Figure S2. Electron density contours of molecular orbitals LUMO, HUMO, HUMO-1 at S_0 geometries of CNDPASDB in the gas phase and ACN.

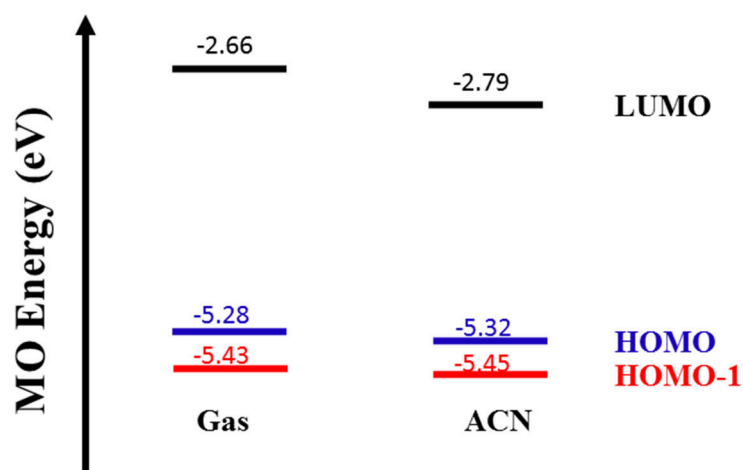


Figure S3. Molecular orbital energy levels at S_0 geometries of CNDPASDB in the gas phase and ACN.

Table S1. Vertical excited energies of **CNDPASDB** in gas phase, TOL, THF and ACN at their optimized ground state geometries at the TD-DFT/CAM-B3LYP/6-31G(d,p) level.

	S_1 (ev)	S_2 (ev)
gas	3.223	3.590
	$f=1.901$	$F=0.001$
	HOMO→LUMO (72%)	HOMO-1→LUMO (66%)
TOL	3.1347	3.4873
	$f=2.0181$	$f=0.001$
	HOMO→LUMO (71%)	HOMO-1→LUMO (67%)
THF	3.127	3.475
	$f=1.976$	$f=0.001$
	HOMO→LUMO (71%)	HOMO-1→LUMO (67%)
ACN	3.126	3.474
	$f=1.953$	$f=0.001$
	HOMO→LUMO (70%)	HOMO-1→LUMO (67%)

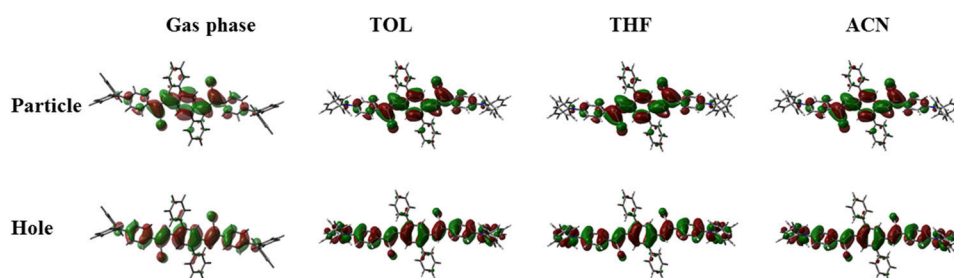


Figure S4. Natural transition orbital pairs describing the lowest singlet excited state in gas phase, TOL, THF, and ACN.

S5. Time-resolved TA spectra in cyclohexane of **CNDPASDB** following 400 nm photoexcitation.

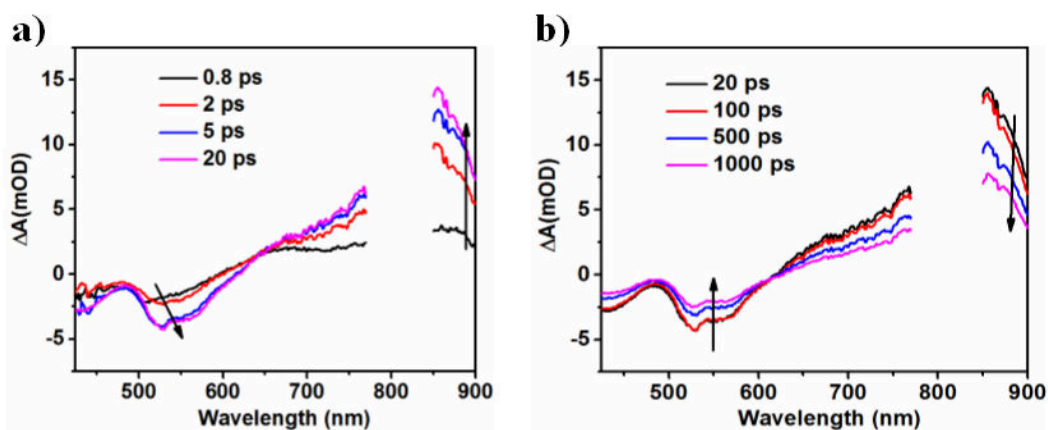


Figure S5. Femtosecond transient absorption spectra of **CNDPASDB** in nonpolar solvent CHX a) 0.8-20 ps and b) 20-1000ps after excitation at 400 nm.

In CHX, there are similar dynamical features with in TOL. While the red-shift of SE peak and spectral narrowing process are presented in the first 20 ps and then all the GSB, ESA and SE bands decay monotonously, which is close to the lifetime of fluorescence.

S6. Lifetime measurement at selected wavelength of CNDPASDB in THF.

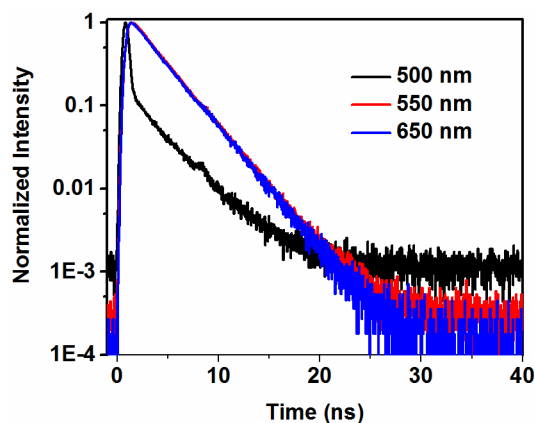
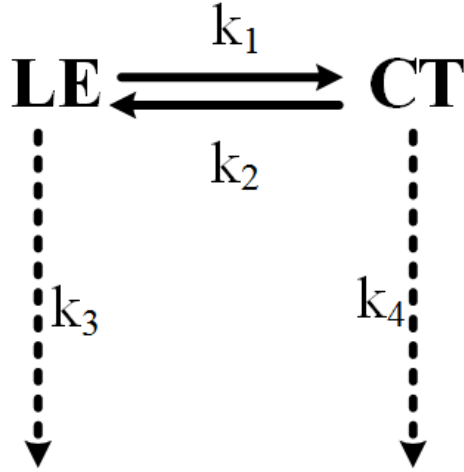


Figure S6. Photoluminescence decay curves of **CNDPASDB** in THF at 500nm, 550 nm and 650 nm.

S7. The coupling deactivation pathways in medium-polarity solvent THF.



For an excited-state equilibrium between LE and CT states, the differential rate equations for the change of concentration of LE and CT state, with time are given by:

$$\frac{dLE}{dt} = -(k_1 + k_3)[LE] + k_2[CT] \quad (\text{S6})$$

$$\frac{dCT}{dt} = -(k_2 + k_4)[CT] + k_1[LE] \quad (\text{S7})$$

The integration of eqs S6 and S7 with the initial boundary condition that only LE is directly excited and populated at time zero: $t=0$, $[LE]=[LE]_0$ and $[CT]=0$, yields the following equations for $[LE]$ and $[CT]$:

$$[LE] = [LE]_0(\alpha_1^{LE} e^{-t/\tau_1} + \alpha_2^{LE} e^{-t/\tau_2}) \quad (\text{S8})$$

$$[CT] = [LE]_0(\alpha_1^{CT} e^{-t/\tau_1} + \alpha_2^{CT} e^{-t/\tau_2}) \quad (\text{S9})$$

The decay times τ_1 and τ_2 and preexponential amplitudes are related to the rate constants include in Scheme 2 according to

$$\alpha_1^{LE} = \frac{\gamma_{LE} - \gamma_2}{\gamma_1 - \gamma_2} \quad (\text{S10})$$

$$\alpha_2^{LE} = \frac{\gamma_1 - \gamma_{LE}}{\gamma_1 - \gamma_2} \quad (\text{S11})$$

Where, $\gamma_1, \gamma_2 = \tau_1^{-1}, \tau_2^{-1} = \frac{1}{2} \left\{ (\gamma_{LE} + \gamma_{CT}) \pm [(\gamma_{LE} - \gamma_{CT})^2 + 4k_1k_2]^{1/2} \right\}$

With $\gamma_{LE} = k_1 + k_3$ and $\gamma_{CT} = k_2 + k_4$.